

Cosmological constraints from COMBO-17 using 3D weak lensing

T. D. Kitching^{*1}, A. F. Heavens¹, A. N. Taylor¹, M. L. Brown¹,

K. Meisenheimer², C. Wolf³, M. E. Gray⁴, D. J. Bacon¹

¹*SUPA[†], Institute for Astronomy, University of Edinburgh, Royal Observatory, Blackford Hill, Edinburgh, EH9 3HJ, U.K.*

²*Max-Planck-Institut für Astronomie, Königsstuhl 17, 69117 Heidelberg, Germany*

³*University of Oxford, Denys Wilkinson Building, Department of Physics, Wilkinson Building, Keble Road, Oxford OX1 3RH, U.K.*

⁴*School of Physics and Astronomy, University of Nottingham, Nottingham, NG7 2RD, U.K.*

22 July 2018

ABSTRACT

We present the first application of the 3D cosmic shear method developed in Heavens et al. (2006) and the geometric shear-ratio analysis developed in Taylor et al. (2006), to the COMBO-17 data set. 3D cosmic shear has been used to analyse galaxies with redshift estimates from two random COMBO-17 fields covering 0.52 square degrees in total, providing a conditional constraint in the (σ_8, Ω_m) plane as well as a conditional constraint on the equation of state of dark energy, parameterised by a constant $w \equiv p_{\text{de}}/\rho_{\text{de}}c^2$. The (σ_8, Ω_m) plane analysis constrained the relation between σ_8 and Ω_m to be $\sigma_8(\Omega_m/0.3)^{0.57 \pm 0.19} = 1.06_{-0.16}^{+0.17}$, in agreement with a 2D cosmic shear analysis of COMBO-17. The 3D cosmic shear conditional constraint on w using the two random fields is $w = -1.27_{-0.70}^{+0.64}$. The geometric shear-ratio analysis has been applied to the A901/2 field, which contains three small galaxy clusters. Combining the analysis from the A901/2 field, using the geometric shear-ratio analysis, and the two random fields, using 3D cosmic shear, w is conditionally constrained to $w = -1.08_{-0.58}^{+0.63}$. The errors presented in this paper are shown to agree with Fisher matrix predictions made in Heavens et al. (2006) and Taylor et al. (2006). When these methods are applied to large datasets, as expected soon from surveys such as Pan-STARRS and VST-KIDS, the dark energy equation of state could be constrained to an unprecedented degree of accuracy.

Key words: cosmology: observations - gravitational lensing

1 INTRODUCTION

This paper presents the first application of 3D weak lensing techniques developed in Heavens (2003), Heavens et al. (2006), Jain & Taylor (2003) and Taylor et al. (2006) to data. The data used is the COMBO-17 survey (Wolf et al. 2001; Wolf et al., 2004) which is a multi-band photometric survey with exceptional image quality and is ideal for a 3D weak lensing study. The power of these methods is cosmological parameter estimation, focussing especially on measuring the equation of state of dark energy which appears to be responsible for the acceleration of the Universe.

The case that the isotropic expansion of the Universe is accelerating is now convincing. The acceleration can be attributed to the effect of a negative pressure component, dark

energy, which accounts for approximately 70% of the mass-energy of the Universe. However the identity of dark energy is entirely unknown. The nature of dark energy may be ultimately determined by establishing its equation of state, parameterised by

$$w \equiv p_{\text{de}}/\rho_{\text{de}}c^2. \quad (1)$$

A cosmological constant has $w = -1$, a dynamical dark energy such as quintessence may have $w \neq -1$. Note that in general w may be a function of redshift, z . This study attempts to use 3D weak lensing to constrain w (where we have assumed that w is a constant), for the first time. It is based on only 0.78 square degrees of data, and is essentially a proof of concept in preparation for much larger surveys such as VST-KIDS, Pan-STARRS (Kaiser, 2005) or the Dark Energy Survey (Wester, 2005) which could lead to very accurate measurements of w and its redshift evolution.

We also present constraints on the amount of matter

* tdk@roe.ac.uk

† The Scottish Universities Physics Alliance

in the Universe Ω_m and the clustering of matter, parameterised by σ_8 , the rms of the fractional mass density fluctuations in spheres of radius $8h^{-1}$ Mpc. Weak lensing has already proven to be a powerful probe of both Ω_m and σ_8 , using 2D weak lensing techniques. We show that a fully 3D shear analysis can also place tight constraints on the matter content and clustering.

Other surveys have used weak lensing data to constrain cosmological parameters using 2D and tomographic tests. Most recently Semboloni et al. (2006), Hoekstra et al. (2006), Schrabback et al. (2006) and Hettterscheidt et al. (2006) have all constrained σ_8 , Ω_m and Ω_{de} , though all these surveys cover a much larger area than COMBO-17. Hoekstra et al. (2006) use the first data release of the CFHTLS Wide survey, which covers 22 square degrees in the i' -band, to constrain $\sigma_8 = 0.85 \pm 0.06$ for $\Omega_m = 0.3$, the full CFHTLS survey will cover 170 square degrees in 5 photometric bands. Semboloni et al. (2006) use the CFHTLS Deep data which covers 2.34 square degrees in (u^*, g', r', i', z') to constrain $\sigma_8 = 0.89 \pm 0.06$ for $\Omega_m = 0.3$. Semboloni et al. (2006) also combine with Hoekstra et al. (2006) to place an upper bound on w , marginalizing over Ω_m , of $w < -0.8$.

COMBO-17 has the best and most reliable photometric redshifts to date, due to the large number of bands, and so is ideal as a survey to test the 3D weak lensing constraints. COMBO-17 is then ideal for this proof of concept, however as shown in Heavens et al. (2006) and Taylor et al. (2006) when much larger survey areas are available, a 5-band large area survey could constrain the dark energy equation of state much better than correspondingly smaller area 17-band survey.

The first 3D weak lensing technique used in this paper is a 3D cosmic shear analysis which analyses the full 3D cosmic shear field using a spherical harmonic expansion, proposed in Heavens (2003) and developed in Castro et al. (2005) and Heavens et al. (2006). The second technique, suggested by Jain & Taylor (2003), is a geometric shear-ratio analysis which takes the ratio of tangential shears around galaxy clusters, developed in Taylor et al. (2006). Both of these analyses are applied to the data available. We use 3D cosmic shear to place conditional constraints on w and to place conditional constraints in the (σ_8, Ω_m) plane using the two random fields. The A901/2 field is centered on a known supercluster, so we use the geometric test on this field to place a conditional constraint on the dark energy equation of state parameter w . This separation of the data allows for a combination of the two methods in the constraint of w .

The results of this paper are a proof of method for these techniques. Heavens et al. (2006) and Taylor et al. (2006) show that in order to constrain the dark energy equation of state to $\Delta w \approx 0.01$ large and deep photometric surveys will be needed. The errors on the results in this paper are compared to predictions made using the Fisher matrix formalism used in Heavens et al. (2006) and Taylor et al. (2006). Brown et al. (2003) have already applied 2D weak lensing to the COMBO-17 data set to constrain the (σ_8, Ω_m) plane. The results presented in this paper using the fully 3D cosmic shear analysis on the same data set, should be in approximate agreement (but do slightly better than) a 2D analysis. It should also be noted that in order to constrain the dark energy equation of state one necessarily needs 3D methods. To determine whether dark energy is a field or a manifesta-

tion of modified gravity (e.g. Ishak et al., 2006), one needs methods can probe the expansion history of Universe, as is the case with the geometric shear-ratio analysis, or both the expansion history and the growth of structure as is the case in the 3D cosmic shear analysis.

The structure of this paper is as follows: firstly the COMBO-17 data set will be introduced and discussed in Section 2, the application of the 3D cosmic shear analysis to the two random fields will be presented in Section 3, the geometric shear-ratio analysis and the results of applying the method to the A901/2 field will be presented in Section 4. The constraints from the A901/2 field (using the geometric shear-ratio analysis) and the constraints from the two random fields (using the 3D cosmic shear analysis) will be combined in Section 5. Conclusions will be presented in Section 6.

2 THE COMBO-17 SURVEY

The COMBO-17 survey is a 17-band photometric redshift survey with gravitational lensing quality R-band data (Wolf et al., 2001; Wolf et al., 2004). The survey consists of five fields each covering 0.26 square degrees. All of the fields were observed using the Wide-Field Imager (WFI) at the MPG/ESO 2.2m telescope on La Silla in Chile, with a 4×2 array of 2048×4096 pixel CCDs, each pixel subtending 0.238 arcseconds.

In this paper we will use three of the COMBO-17 fields, which were observed and reduced earlier than the remaining two, and for which there are redshift estimates and a shear catalogues available. One of the fields used, the A901/2 field, is centred on the Abell 901/2 supercluster which has previously been analysed in 2D by Gray et al (2002) and in 3D by Taylor et al. (2004). The A901/2 supercluster consists of three smaller clusters; A901a, A901b, A902, all at a redshift of $z \approx 0.16$. It should be noted that supercluster refers to a ‘web of clusters’, the individual clusters are much smaller $\sim 10^{14} M_\odot$ (see Taylor et al., 2004) than large strong lensing clusters for example A1689. For an individual cluster the fractional error on w should decrease as the mass of the cluster increases. However in a large area survey there should be many more low and medium mass clusters than large clusters so that the constraint on w is dominated by the numerous medium mass clusters; for a detailed discussion see Taylor et al. (2006).

The COMBO-17 survey also observed a randomly selected area of sky, and a relatively empty, but well observed area. The S11 field was a randomly selected area of sky, that contains a moderately large cluster Abell 1364 at a redshift of $z \approx 0.11$. The CDFS field was chosen to overlap the Chandra Deep Field South, a relatively ‘empty’ region of sky containing no significant galaxy clusters. We only used galaxies with reliable photometric redshifts and with an R magnitude of $R \leq 24$.

2.1 Photometric Redshifts

Each of the COMBO-17 fields was observed in 17 different filters, with the intention of obtaining object classification and accurate photometric redshifts. In order to provide reliable redshifts, the filter set included five broad-band filters

(*UBVRI*) and 12 medium-band filters from 350 to 930 nm. This observing strategy allows simultaneous estimates of Spectral Energy Distribution (SED) classifications and photometric redshifts from empirically-based templates. Wolf et al. (2001) describe in detail the photometric redshift estimation methods used to obtain typical accuracies of $\sigma_z \approx 0.05$ for galaxies throughout $0 < z < 1$. We fit an empirical line to the data such that

$$\sigma_z(z) = 0.03(1+z)^{1.5}, \quad (2)$$

this $\sigma_z(z)$ is used in the likelihood analysis. It should be noted that the parameter constraints are not sensitive to the exact functional form of $\sigma_z(z)$.

2.2 Shear Measurements

Throughout the observing campaign the *R* filter was used in best seeing conditions, in order to provide a deep *R*-band image from which to measure the gravitational shear. Gray et al. (2002) discuss the procedure used to reduce the *R* band imaging data, which totalled 21 hours for the three fields used. As described by Gray et al. (2002) and Brown et al. (2003) the 352 individual chip exposures for each field were registered using linear astrometric fits, with a 3σ rejection of bad pixels and columns.

The Kaiser, Squires & Broadhurst (1995; KSB) weak lensing measurement method was applied, using the *imcat* shear analysis package, to the reduced images (see Gray et al., 2002; Brown et al., 2003). This resulted in a catalogue of galaxies with centroids and shear estimates throughout the fields, corrected for the effects of anisotropic smearing and point spread function (PSF) circularisation. The photometric redshift estimates were appended to this catalogue for each galaxy from the standard COMBO-17 analysis of the full multi-colour dataset. Of the 37,243 galaxies in the shear catalogue, 36% have a reliable photometric redshift, the remainder being fainter than the $R = 24$ reliability limit of the redshift survey. The requirement for the 3D lensing study, that the redshift of each galaxy be known, clearly results in an immediate reduction of available galaxies. It is apparent that most of the background sample is composed of galaxies that are small, and fainter than the magnitude limit of the redshift survey. These catalogues are the raw data used in this analysis. Brown et al. (2003) also include galaxies without assigned redshifts into their analysis, this can also be done in the case of 3D weak lensing however since this paper is a proof of concept for the 3D weak lensing methods the galaxies without redshifts will be left out of this analysis.

3 THE 3D COSMIC SHEAR ANALYSIS

We have applied the 3D cosmic shear method to the CDFS and S11 fields of COMBO-17 in order to constrain w and jointly constrain σ_8 and Ω_m . Bacon et al. (2005) analysed COMBO-17 using a real-space 3D cosmic shear method to constrain the evolution of dark matter clustering. The results presented in this Section are based on the methods outlined in Heavens et al. (2006).

3.1 3D Cosmic Shear Likelihood

The statistics we choose to work with are the transforms of the galaxy ellipticities. The transforms are defined, for a given radial k -mode and angular ℓ -mode, by summing over all galaxies g , each at a redshift z and angular position θ_g , in a given field catalogue

$$\hat{\gamma}_i(k, \ell) = \sqrt{\frac{2}{\pi}} \sum_g e_i^g k j_\ell(k r_g^0) X_\ell e^{-i\ell \cdot \theta_g} W(z). \quad (3)$$

The hat indicates that these are estimators of the transform of the shear field, but the relationship is not direct as the number density of sources is non-uniform.

g refers to the galaxies in the sample, e_i^g is the i component of the complex ellipticity of the galaxy related to the weak shear γ_i^g and the intrinsic ellipticity of the galaxy by $e_i^g = e_i^g(\text{intrinsic}) + \gamma_i^g$. r_g^0 denotes the comoving distance to a galaxy calculated from the photometric redshift of the galaxy by assuming a fiducial cosmology. The $j_\ell(z)$ are spherical Bessel functions. $W(z)$ is a weighting function which we set to $W(z) = 1$ for the remainder of this paper; for an investigation of the effect of changing the weighting scheme see Heavens et al. (2006). The X_ℓ factor is introduced as a result of relating the potential to the shear field $\gamma(\mathbf{r}) = \frac{1}{2} \bar{\partial} \bar{\partial} \phi(\mathbf{r})$ (see Heavens et al., 2006) and is given by

$$X_\ell \equiv \frac{(\ell_y^2 - \ell_x^2) + 2i\ell_x \ell_y}{\ell^2}. \quad (4)$$

The expansion using spherical Bessel functions is natural for a flat universe. For non-flat universes, the appropriate functions are ultra-spherical Bessel functions $\Phi_\beta^\ell(y)$, but in the $\ell \gg 1$ and $k \gg (\text{curvature scale})^{-1}$ régime these are well approximated by ordinary Bessel functions $\Phi_\beta^\ell(y) \rightarrow j_\ell(kr)$ (Abbott and Schaefer, 1986; Zaladarriga and Seljak, 2000).

For each e_i^g component there is a real and imaginary estimator (via the $X_\ell e^{-i\ell \cdot \theta_g}$ factor) so that the whole data vector used in the likelihood analysis consists of four independent vectors at each k and ℓ : $\hat{\gamma}_1^R, \hat{\gamma}_1^I, \hat{\gamma}_2^R, \hat{\gamma}_2^I$, where the R superscript denotes the real part of the $\hat{\gamma}_i$ estimator and I the imaginary part. Note that this is for a given ℓ -mode.

The fiducial cosmology, denoted by the superscript 0, is in this case chosen to have $\Omega_m = 0.3$, $\Omega_{de} = 0.7$, $\Omega_b = 0.04$, $h \equiv H_0/100 \text{ kms}^{-1} \text{ Mpc}^{-1} = 0.71$, $\sigma_8 = 0.8$, $w = -1.0$; we also set the scalar spectral index to be $n_s = 1.0$ and its running $\alpha_n = 0.0$. The choice of the fiducial cosmology does not affect the results presented in this paper, as long as the measured shear estimates and theoretical calculations use the same fiducial cosmology to calculate the transform coefficients. This fiducial cosmology simply acts, via the spherical Bessel functions, to weight the shear values in a particular way. The cosmological dependence comes from the shear values themselves, γ_i^g , the cosmological dependence of the calculated covariance matrices come from modelling the shear-shear covariance. We tested a variety of fiducial models and the results were indeed unaffected.

Note that the average value of $\hat{\gamma}_i(k, \ell)$ is zero, so that information on the cosmological parameters comes from the dependence of the signal part of the covariance matrix C i.e. we adjust the parameters until the *covariance* of the model matches that of the data. This was the approach of Heavens and Taylor (1995); Ballinger, Heavens and Taylor (1995); Tadros et al. (1995); Percival et al. (2004) in analy-

sis of large-scale galaxy data. The details of the covariance matrix derivation are given in Heavens et al. (2006), where the covariance matrix is given as the sum of signal and noise terms $C = S + N$. The signal part of the covariance of $\gamma(k, \ell)$ for a survey of size $\Delta\theta \times \Delta\theta$ can be written as

$$\begin{aligned} S &= \langle \gamma(k, \ell) \gamma^*(k', \ell') \rangle_S \\ &= \int \frac{d^2 \tilde{\ell}}{(2\pi)^2} Q(\ell, \ell', \tilde{\ell}, k, k') |X_{\tilde{\ell}}|^2 \\ &\quad \int_{-\Delta\theta/2}^{\Delta\theta/2} d^2 \theta e^{-i(\ell - \tilde{\ell}) \cdot \theta} \int_{-\Delta\theta/2}^{\Delta\theta/2} d^2 \theta' e^{-i(\ell' - \tilde{\ell}) \cdot \theta'}. \end{aligned} \quad (5)$$

The Q matrix is given by

$$Q(\ell, \ell', \tilde{\ell}, k, k') = \frac{9\Omega_m^2 H_0^4}{4\pi^2 c^4} \int \frac{d\tilde{k}}{\tilde{k}^2} G(\ell, \tilde{\ell}, k, \tilde{k}) G(\ell', \tilde{\ell}, k', \tilde{k}) \quad (6)$$

where

$$G(\ell, \tilde{\ell}, k, \tilde{k}) \equiv k \int dz dz_p \bar{n}_z(z_p) p(z_p|z) U(\tilde{\ell}, r, \tilde{k}) j_\ell(kr^0) \quad (7)$$

where z_p is an integral over redshift given an assumed cosmology, and the integral over z uses the cosmology to be tested. $\bar{n}_z(z)$ is the predicted number density of objects as a function of redshift which is measured from the survey in question. $p(z_p|z)$ is a probability distribution in redshift which, by convolving with the redshift distribution, takes into account the uncertainty in redshift. We assume a Gaussian probability distribution with the width being the measured photometric redshift as a function of redshift (see Section 2.1).

The U matrix used in equation (7) is

$$U(\tilde{\ell}, r, \tilde{k}) \equiv \int_0^r d\tilde{r} \frac{F_K(r, \tilde{r})}{a(\tilde{r})} \sqrt{P_\delta(k; \tilde{r})} j_{\tilde{\ell}}(k\tilde{r}), \quad (8)$$

where $P_\delta(k; r)$ is the matter power spectrum for the cosmology to be tested. We compute the nonlinear power spectrum using the fitting formulae of Smith et al. (2003), based on linear growth rates given by Linder and Jenkins (2003). $F_K(r, r') = (1/r' - 1/r)$ for a flat Universe (assumed in this paper) and $a(r)$ is the dimensionless scale factor.

The integrals over θ in equation (5) can be evaluated so that

$$S = \int \frac{d^2 \tilde{\ell}}{(2\pi)^2} Q(\ell, \ell', \tilde{\ell}, k, k') |X_{\tilde{\ell}}|^2 \mathcal{F}(\ell, \ell', \tilde{\ell}), \quad (9)$$

where

$$\mathcal{F}(\ell, \ell', \tilde{\ell}) \equiv \prod_{i=x,y} \frac{4}{(\tilde{\ell} - \ell)_i (\tilde{\ell} - \ell')_i} \sin \left[(\tilde{\ell} - \ell)_i \frac{\Delta\theta}{2} \right] \sin \left[(\tilde{\ell} - \ell')_i \frac{\Delta\theta}{2} \right] \quad (10)$$

$i = x, y$ represents the x and y components of a Cartesian coordinate system for a survey.

The shot noise part of the covariance matrix is calculated by assuming a Poisson sampling an underlying smooth density field and is given by

$$\begin{aligned} N &= \langle \hat{\gamma}_\alpha(k, \ell) \hat{\gamma}_\beta^*(k', \ell') \rangle_{SN} \\ &= \frac{\sigma_\epsilon^2 \Delta\Omega}{4\pi^2} \int dz \bar{n}_z(z) k j_\ell(kr^0) k' j_{\ell'}(k'r^0) \delta_{\alpha\beta}^K \delta_{\ell\ell'}^K \end{aligned} \quad (11)$$

where $\Delta\Omega = \Delta\theta \times \Delta\theta$. σ_ϵ is measured from the data, for the CDFS field $\sigma_\epsilon = 0.19$ and for the S11 field $\sigma_\epsilon = 0.22$.

For large surveys the calculation simplifies as $\mathcal{F} \rightarrow (\Delta\theta)^2 \delta_{\ell\ell'}^K \delta_{\ell'\ell}^K$ (see equation 10) and the covariance matrix becomes diagonal in (ℓ, ℓ') . For COMBO-17, the survey is small so that it is necessary to compute the integral in equation (9) accurately using the full $\mathcal{F}(\ell, \ell', \tilde{\ell})$. We do this for the diagonal components of Q , but we make an approximation by ignoring the off-diagonal components. Improvement on this would involve computing the full covariance resulting in vast computational expense, which is not really warranted by the size of the dataset. All correlations between k -modes, for any given ℓ -mode are fully taken into account.

We assume then that the distribution of ℓ -modes can be represented by a multivariate Gaussian. The likelihood function for a given ℓ and set of cosmological parameters $\{\theta_\alpha\}$ is given by

$$\begin{aligned} -2 \ln L_\ell(\theta_\alpha | \mathbf{D}) &= \sum_{A=\{R,I\}} \sum_{i=\{1,2\}} N_i^A \ln(2\pi) \\ &\quad + \ln(|C_{i,\ell}(k, k')^{AA}|) \\ &\quad + \sum_{kk'} \hat{\gamma}_\ell^A(k) (C_{i,\ell}^{-1}(k, k'))^{AA} \hat{\gamma}_\ell^{A,T}(k') \end{aligned} \quad (12)$$

where $A = \{R, I\}$ is a sum over the real and imaginary estimators and $i = \{1, 2\}$ is a sum over the γ_1 and γ_2 shear components. N_i^A is the number of k -modes in the $N_i^A \times N_i^A$ covariance matrix $C_{i,\ell}(k, k')^{AA}$. The log-likelihood is then summed over each independent $\ell = (\ell_x, \ell_y)$ mode. Note that since we have four independent data vectors, two real and imaginary pairs, we only investigate the range $\ell_x \geq 0$ to avoid double counting.

The ℓ and k ranges and resolutions used are as follows. In integrating over $\tilde{\ell}$ in equation (5) we found that the signal converges at $\Delta\tilde{\ell}_i = 100$ and for the range $(\ell_i - 1500) < \tilde{\ell}_i < (\ell_i + 1500)$ where $i = x, y$. The k resolution used was $\Delta k = 2 \times 10^{-3} \text{ Mpc}^{-1}$, as it was found that the signal part of the covariance matrix converges at $\Delta k \approx (2\pi/r_{\text{max}}) \approx 2 \times 10^{-3} \text{ Mpc}^{-1}$ where r_{max} is the distance corresponding to a maximum redshift of $z \approx 1$. The k range used was $0.01 < k < 1.5 \text{ Mpc}^{-1}$. The ℓ values available are constrained by the survey geometry, $\ell_i = \frac{2\pi n}{\Delta\Theta}$ where n is an integer; $\ell_1 = 671$. We tested the lower ℓ limit and found no change in the cosmological constraints by using $\ell_1 = 700$ instead, showing that these results are robust to the details of the lower ℓ range used. We use all modes with $|\ell| \leq 2500$ to avoid the highly non-linear régime in which baryonic physics may have a significant effect (Zhan & Knox, 2004; White, 2004) on the power spectrum. We calculate non-linear effects accurately using the fitting formula of Smith et al. (2003) for the matter power spectrum. The use of a Gaussian likelihood is an approximation. The scales probed by the technique currently extend significantly into the non-linear régime, but the integral nature of lensing is expected to make the shear more Gaussian (Hu & White, 2001). However, it remains to be tested with simulations whether the Gaussian approximation leads to significant error. This will be the subject of future work. Note that since $\ell = (\ell_x, \ell_y)$ the ℓ range used corresponds to 26 independent ℓ -modes.

The use of spherical Bessel functions in the coefficients used means that, for any given ℓ -mode, there is a range of k for which the signal is zero up until a particular value of $k \approx |\ell|/r_{\text{max}}$ (see Castro et al., 2005). These zero modes result in

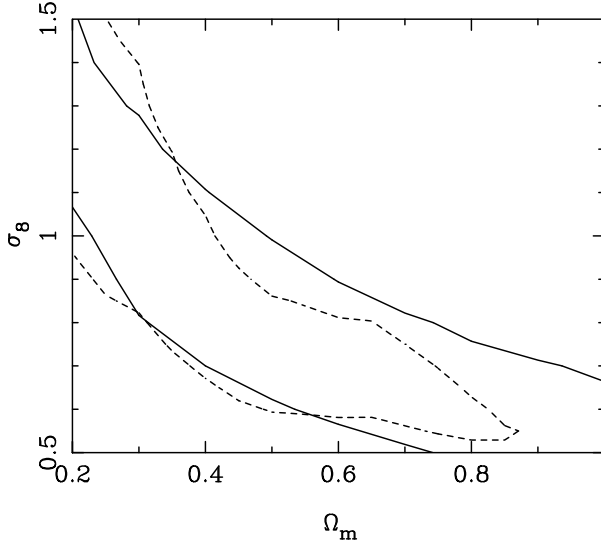


Figure 1. The solid lines show the two-parameter 1- σ conditional constraints in the (σ_8, Ω_m) plane from applying the 3D cosmic shear analysis to the CDFS and S11 fields only. The dashed contours show the two-parameter 1- σ conditional constraints from the Brown et al. (2003) analysis using 50% more fields: CDFS, S11 and A901/2.

singular covariance matrices, however this behaviour can be taken into account using the prescription given in Appendix A.

3.2 3D Cosmic Shear Results

This Section presents the result of applying the 3D cosmic shear analysis to the CDFS and S11 fields. The results will be compared with the Fisher matrix analysis of Heavens et al. (2006) and with the 2D cosmic shear analysis of Brown et al. (2003). Unless otherwise stated the fiducial cosmology that will be assumed throughout this Section is $\Omega_m = 0.3, \Omega_{de} = 0.7, \Omega_b = 0.04, h = 0.71, \sigma_8 = 0.8, w = -1.0, n_s = 1.0, \alpha_n = 0.0$, any constraints for particular parameters are conditional on these values.

Figure 1 shows the two-parameter 1- σ contours from applying the 3D cosmic shear analysis to the CDFS and S11 fields only. The dashed line in Figure 1 shows the two-parameter 1- σ contours from Brown et al. (2003) where a traditional 2D cosmic shear analysis was performed on all three COMBO-17 fields, CDFS, S11 and A901/2 using only galaxies with accurate redshifts. It can be seen that the 3D cosmic shear analysis constrains a very similar area in the (σ_8, Ω_m) plane, particularly at the concordance values of σ_8 and Ω_m using less than two thirds the number of galaxies used in the 2D analysis (since the A901/2 field contains more galaxies than the CDFS and S11 only 63% of the galaxies used in the 2D analysis have been analysed).

A common way to express the constraint in the (σ_8, Ω_m) plane is to constrain the parameterisation $\sigma_8(\Omega_m/0.3)^\beta = \alpha$, where β expresses the curvature of the constraint and α the normalisation of the curve. The 3D cosmic shear analysis

constrains these parameters to be

$$\begin{aligned} \alpha &= 1.06^{+0.17}_{-0.16} \\ \beta &= 0.57^{+0.19}_{-0.19} \end{aligned} \quad (13)$$

these are consistent with the constraints from the 2D analysis of Brown et al. (2003). It should be noted however that Brown et al. (2003) have a maximum ℓ limit of $\sim 10,000$, so that they use substantially more modes in the angular direction. Also, their main result of $\sigma_8(\Omega_m/0.3)^{0.49} = 0.72^{+0.08}_{-0.09}$ included galaxies with unknown redshifts, the result shown (dashed line in Figure 1) is their result when considering galaxies with only reliable redshift estimates. Since the range in ℓ -modes and the number of galaxies are different in the two analyses this comparison cannot make any conclusions on the relative merit of the two techniques. It is sufficient to say that our results agree with Brown et al. (2003) when we include the same sort of data i.e. from an analysis in which the majority of the galaxies were the same the results are consistent with one another.

The high value of σ_8 is unexpected for the CDFS and S11 fields, the CDFS result on its own favours a lower σ_8 (with substantially increased error contours), so that the cluster in the S11 field appears to increase the most likely value of σ_8 . Also the effect of not including galaxies with photometric redshifts appears to increase the most likely clustering value in Brown et al. (2003) (compare Figures 19 and 20 in Brown et al., 2003). Since we do not include galaxies for which a redshift is unknown we may expect to find a high clustering value in a similar way to Brown et al. (2003). We only used galaxies with reliable redshifts since this paper is a proof of concept for the 3D weak lensing methods, however galaxies with unknown redshifts could also be included in this analysis.

The Fisher matrix calculations in Heavens et al. (2006) can be used to predict the estimated uncertainties from this analysis. Fisher matrix predictions, by construction, predict Gaussian likelihood surfaces, the curved constraint shown here highlights one limitation of the Fisher matrix technique to predict uncertainties when the errors are so large. However, using the techniques outlined in Heavens et al. (2006), we predict, for two COMBO-17 fields, a conditional constraint of $\Delta\sigma_8 = 0.19$ (assuming $\Omega_m = 0.3$). This is in agreement with the measured conditional error of $\sigma_8(\Omega_m = 0.3) = 1.05 \pm 0.20$, highlighting that the predictions made in Heavens et al. (2006) are reliable. The values used in the Fisher matrix calculation were an area of $A = 0.52$ square degrees, to a median redshift of $z_{\text{median}} = 0.8$ using the photometric redshift error given in equation (2).

Figure 2 shows the conditional constraint on w from the CDFS and S11 field only using the 3D cosmic shear analysis. The constraint is asymmetric in that the range $w < -1$ is more likely than $w > -1$. This is due to the fact that values of $w < -1$ represent dark energy scenarios in which the dark energy density is less in the past, so it is more difficult to constrain its equation of state. Semboloni et al. (2006) also found a similar asymmetric constraint when using weak lensing tomography applied to the CFHTLS survey. The conditional constraint on w is

$$w = -1.27^{+0.64}_{-0.70}. \quad (14)$$

This result is consistent with other observations (for example Spergel et al., 2006) and with a cosmological constant model

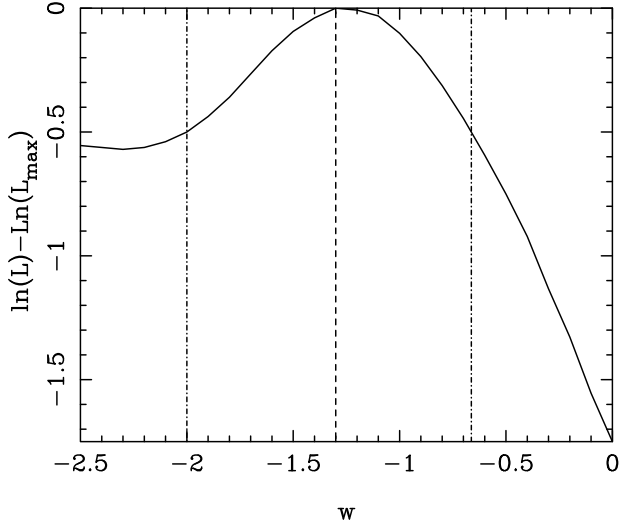


Figure 2. The one-parameter maximum likelihood constraint on w from the CDFS and S11 fields using the 3D cosmic shear analysis. The dashed line shows the most likely value and the dot-dashed show the one-parameter $1\text{-}\sigma$ constraints.

for dark energy. The Fisher matrix calculations, presented in Heavens et al. (2006) predict a conditional error on w from two COMBO-17 fields to be $\Delta w = 0.62$ which is in agreement with the constraints presented here.

Typical reduced χ^2 values for a given ℓ -mode in the CDFS and S11 fields analyses are $\chi_{CDFS}^2 \approx 1.01$ and $\chi_{S11}^2 \approx 0.98$, the number of degrees of freedom for a given ℓ -mode are the corresponding number of non-singular k -modes used in the analysis, typically ~ 600 for an average ℓ -mode. The range of χ^2 values are consistent with a good fit to the data.

4 THE GEOMETRIC SHEAR-RATIO ANALYSIS

We have applied the geometric shear-ratio analysis to the A901/2 field of the COMBO-17 survey in order to conditionally constrain w , and compare the measured constraint with the predicted constraint from a Fisher matrix calculation. The results presented in this Section are an extension and use of the methods outlined in Taylor et al. (2006).

4.1 Geometric Shear-Ratio Likelihood

To implement the geometric shear-ratio analysis, we first selected the peaks in the convergence field of the three clusters, A901a, A901b and A902. Taylor et al. (2004) have shown that there is a fourth cluster, CB1, in this field, which lies behind A902 at a redshift of $z = 0.42$. Here we shall ignore the contribution of this cluster, although this will in principle bias our results slightly. To estimate the effect of the bias the CB1 cluster increases the tangential shear, at $z \gtrsim 0.4$, by $\delta\gamma_t \lesssim 0.02$ (see Taylor et al., 2004). Using the simple error formula from Taylor et al. (2006) this increase in tangential shear may bias the value of w by $\delta w \lesssim +0.03$.

We use the positions of the centre for each cluster given by Taylor et al. (2004), in which the tangential shear around

each cluster is used to determine the 3D position and mass of the clusters. We averaged the tangential shear in annuli around each cluster in a series of redshift bins, following Taylor et al. (2004; see Figure 3), the width of the redshift bins is equal to the photometric redshift error at the redshift of the bin using the result from Section 2.1. The lensing signal from a cluster is given by the tangential shear

$$\gamma_t = -[\gamma_1 \cos(2\varphi) + \gamma_2 \sin(2\varphi)], \quad (15)$$

for a given redshift bin. The error on the tangential shear was estimated by the orthogonal shear signal

$$\gamma_\times = [-\gamma_1 \sin(2\varphi) + \gamma_2 \cos(2\varphi)]. \quad (16)$$

Since a lensing cluster induces a tangentially aligned shear signal, any orthogonal component is assumed to be due to noise. In this case we define a polar coordinate system about the cluster centre and assume a circularly-symmetric mass profile, which should produce a purely tangential signal. Under these assumptions any orthogonal component is taken to be due to measurement error, as opposed to deviations from circular symmetry in the lens (which can also produce an orthogonal component in the circular coordinate system chosen about the cluster center). The tangential shear in each angular and redshift bin was then fitted with a least-square fit to a singular isothermal sphere (SIS) profile;

$$\gamma_{t,SIS}(\theta, z) = \frac{1}{2\theta} \theta_E(z). \quad (17)$$

$\theta_E(z)$ is the Einstein ring radius which parameterises the amplitude of the tangential shear as a function of source redshift. Note that the assumption of a SIS is not necessary, in the case of a large data set the average tangential shear in an aperture could be measured directly, and the orthogonal shear component for the error, with no assumption on the radial tangential shear profile made. Since this data set consists of only three small clusters the SIS was adopted so that a signal could be measured, and for the radii from the centre of the clusters probed should be an adequate approximation.

Here D denotes data and R is the theoretical estimate for the shear ratio, dependent on cosmology. The theoretical ratio of shears, R_{ij} for a pair of redshift bins could then be estimated by

$$R_{ij} = \frac{\theta_E(z_i)}{\theta_E(z_j)} = \frac{(r_{\text{lens}} - r_i)/r_i}{(r_{\text{lens}} - r_j)/r_j} \quad (18)$$

where r is the predicted comoving distance for a given cosmology. The data is simply the ratio of tangential shears

$$D_{ij} = \frac{\gamma_t(z_i)}{\gamma_t(z_j)}. \quad (19)$$

The measured ratio D_{ij} and the calculated ratio R_{ij} are then used in the likelihood function, summing over all pair-pair configurations, given by equation

$$-2 \ln L_c(\Omega_{de}, \Omega_m, w, w_a | \mathbf{D}) = \sum_{\mu, \nu} (R_\mu - D_\mu) [C_{\mu\nu}^{RR}]^{-1} (R_\nu - D_\nu), \quad (20)$$

for a given cluster. The notation for a pair of background bins has been compressed as $\mu = (i, j)$ and $\nu = (m, n)$, and all degenerate pair-pair combinations have been accounted for. The likelihood functions for multiple clusters are multiplied. We can write the covariance matrix for shear ratios

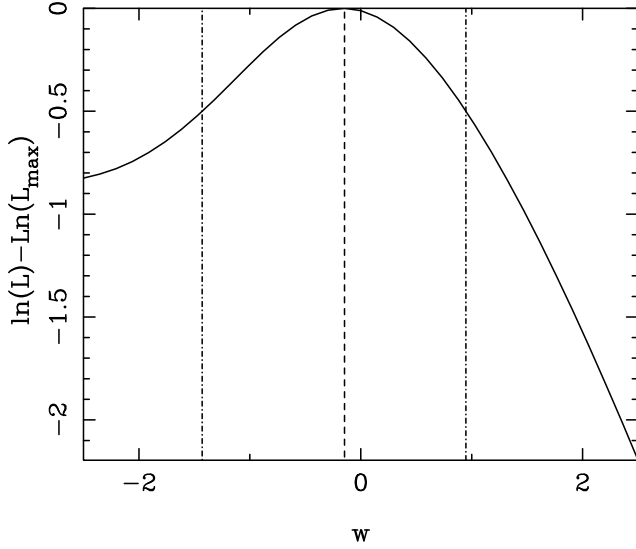


Figure 3. The dark energy geometric shear-ratio analysis applied to the supercluster Abell A901/2. The dashed line marks the maximum likelihood value, the dot-dashed lines show the one-parameter 1- σ limits. Note that the x-axis scale has been extended relative to Figures 2 and 3 to encompass the confidence limits of this analysis.

as

$$C_{\nu\mu}^{RR} \equiv \langle \Delta R_\nu \Delta R_\mu \rangle. \quad (21)$$

The full covariance matrix includes shot noise and cosmic shear terms. For a full description see Taylor et al. (2006).

4.2 Geometric Shear-Ratio Results

The results are shown as a 1D likelihood plot in Figure 3. The result is conditional on $\Omega_m = 0.30$, $\Omega_{de} = 0.70$ and $w_a = 0.0$. The dashed line is our measured most likely value, the dot-dashed lines are the one-parameter 1- σ (68%) confidence limits. Our constraint on w is:

$$w = -0.11_{-1.29}^{+1.05}. \quad (22)$$

The constraint again shows an asymmetry between the $w < -1$ and $w > -1$ regions for the same reason given in the 3D cosmic shears constraint, that $w < -1$ represents a lower dark energy density in the past. The minimum χ^2 value is $\chi_{\min}^2 = 122$ which is consistent with the number of degrees of freedom in the experiment. Given that $z_{\max} \approx 2.0$ and $\Delta z \approx 0.05$ and we analyse $N_{\text{cluster}} = 3$ clusters the predicted $\chi_{\min}^2 = (z_{\max}/\Delta z)N_{\text{cluster}} \approx 120$ so that $\chi_{\text{reduced}}^2 = 1.01$ and should be $\chi_{\text{reduced}}^2 = 1 \pm 0.12$.

The result is consistent with other constraints on w , and the confidence limits allow for most dark energy models. It should be emphasised that this constraint comes from only three small clusters.

The Fisher matrix calculations, in Taylor et al. (2006) predict a conditional constraint on w of $\Delta w = 1.10$ for COMBO-17 which was created by assuming only three clusters at $z = 0.16$ with $M_{\text{cluster}} = 10^{14} M_\odot$. The predicted conditional constraint is approximately the same as the measured constraint, thus verifying the Fisher matrix methodology.

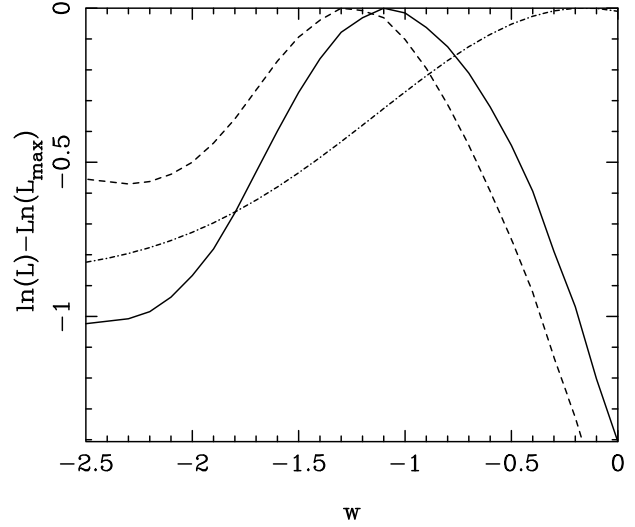


Figure 4. The one-parameter maximum likelihood constraint on w obtained by combining the geometric shear-ratio analysis constraint from A901/2 field and the 3D cosmic shear analysis constraint from the CDFS and S11 fields. The solid line shows the combined constraint, the dashed line shows the 3D cosmic shears constraint shown in Figure 2, the dot-dashed line shows the geometric shear-ratios constraint shown in Figure 3.

5 A COMBINED CONSTRAINT ON w

Since the A901/2 field was analysed separately from the CDFS and S11 fields the geometric shear-ratio analysis constraint can be combined with the constraint from the 3D cosmic shear analysis. Figure 4 shows the result of adding the constraints shown in Figures 2 and 3 from the CDFS and S11 fields and the A901/2 field respectively. The resulting conditional constraint on w is

$$w = -1.08_{-0.58}^{+0.63}. \quad (23)$$

This result demonstrates the value of combining the two techniques that can analyse distinct parts of the data. A region of particularly high density such as the A901/2 field would raise issues of sample bias in a cosmic shear/spectral approach, however the geometric shear-ratio analysis necessarily needs such areas. The effect of adding the geometric shear-ratio analyses constraint is the most likely value becoming more positive, and a slight reduction in the error. The most likely value of $w = -1.08$ is in complete agreement with other observations (for example Semboloni et al, 2006; Spergel et al., 2006) and is close to the value of w expected if dark energy is a cosmological constant. The caveat on this conclusion is that it is conditional on the other cosmological parameters being fixed, and the error on w is still fairly large. Finally it is surprising, given the size of the error, that the maximum likelihood estimate is so close to $w = -1$.

6 CONCLUSION

In this paper we have applied the 3D weak lensing methods introduced in Heavens (2003) and Jain & Taylor (2003) and developed in Heavens et al. (2006) and Taylor et al. (2006)

to data for the first time. We used the COMBO-17 data set, a multi-band photometric survey, ideal for a weak lensing study. We used three of the fields, CDFS, S11 and A901/2 to place conditional constraints on the equation of state of dark energy, w and the (σ_8, Ω_m) plane. The size of the dataset is small so we did not expect accurate constraints and this paper is essentially a proof of concept for the methods. To this end we compute conditional constraints and compare with Fisher matrix predictions. A full analysis of a larger data set should, of course, quote marginal errors.

The first method used was the 3D cosmic shear analysis which uses spherical harmonics to describe the fully 3D shear field. Applying the 3D cosmic shear analysis to the CDFS and S11 field we conditionally constrained an area in the (σ_8, Ω_m) plane described by $\sigma_8(\Omega_m/0.3)^{0.57 \pm 0.19} = 1.06_{-0.16}^{+0.17}$. This is in agreement with Brown et al. (2003) in which a 2D cosmic shear analysis was performed on 50% more data. The application of 3D cosmic shear conditionally constrained the equation of state of dark energy to $w = -1.27_{-0.70}^{+0.64}$.

The second method used was the geometric shear-ratio analysis, which takes the ratio of the tangential shear around galaxy clusters at different redshifts. We applied this analysis to the A901/2 field which contains three small clusters conditionally constraining $w = -0.15_{-1.28}^{+1.07}$.

Combining the constraint on w from the geometric shear-ratio analyses application to the A901/2 field and the 3D cosmic shear constraint from CDFS and S11 we conditionally constrain $w = -1.08_{-0.58}^{+0.63}$. For discussions on the relative merit of the two methods and varying observing strategies see Heavens et al. (2006) and Taylor et al. (2006). These papers also discuss the effects of systematics, number of observing bands used and the effects of the assumed fiducial cosmology.

The constraints presented here do not improve much on our cosmological understanding, they are however in agreement with the currently accepted concordance model of Spergel et al. (2006). The constraint on w from such a small data set is encouraging and, with the warning and caveat that it is a conditional error, it is *a fortiori* consistent with dark energy being a cosmological constant.

In order for these results to become more complete we could marginalize over an increasingly large cosmological parameter set. However this would rapidly result in a loss of any constraint, for such a small survey area, due to degeneracies between the parameters as shown in Heavens et al. (2006) and Taylor et al. (2006). The result errors agree with the Fisher matrix predictions and are a very reliable proof of concept for these methods.

The agreement of the results presented here with the Fisher matrix predictions using the methods presented in Heavens et al. (2006) and Taylor et al. (2006) are a validation of the Fisher matrix framework and an encouraging sign that the predictions made in these papers are robust and accurate. COMBO-17 was an ideal survey upon which to test these 3D weak lensing methods, however with much larger area surveys with fewer observing bands, such as VST-KIDS, Pan-STARRS (Kaiser et al., 2005) or the Dark Energy Survey (Wester, 2005), these techniques could constrain the dark energy equation of state to approximately 1% at a particular redshift.

ACKNOWLEDGMENTS

We would like to thank Patricia Castro for helpful discussions. TDK acknowledges a PPARC studentship. MLB acknowledges the support of a PPARC Fellowship. CW was supported by a PPARC Advanced Fellowship.

REFERENCES

- Abbott L., Schaefer R., 1986, ApJ, 308, 546
Aldering G. et al. 2004, PASP, submitted (astro-ph/0405232)
Bacon D. J., Refregier A. R., & Ellis R. S. 2000, MNRAS, 318, 625
Bacon D. J., et al., 2005, IAUS, 225, 37
Ballinger W., Heavens A.F., Taylor A.N., 1995, MNRAS, 276, 59
Bartelmann M. and Schneider P., 2001, Phys. Rep., 340, 291
Baugh C. and Efstathiou G.P., 1993, MNRAS, 265, 145
Bennett C.L. et al., 2003, ApJS, 148, 1
Bernstein G. 2005, astro-ph/0503276
Brown M., et al., 2003, MNRAS, 314, 100
Castro P.G., Heavens A.F., Kitching T. D., 2003, Phys Rev D72, 023516 (astro-ph/0503479)
Catelan P., Kamionkowski M., Blandford R., 2001, MNRAS, 320, 7
Chevalier M. et al., 2001, Int. J. Mod. Phys. D., 10, 213
Colless M., et al., 2001, MNRAS, 328, 1039
Crittenden R. et al., 2001, ApJ, 559, 552
Croft R.A.C. and Metzler C.A., 2002, ApJ, 545, 561
Croft R.A.C. et al. 2002, ApJ, 581, 20
Fisher K., Scharf C., Lahav O., 1994, MNRAS, 266, 219
Gnedin N., Hamilton A.J.S., 2002, MNRAS, 334, 107
Gray M. et al., 2002, ApJ, 568, 141
Gray M. et al., 2004, MNRAS, 347, 73
Heavens A.F., 2003, MNRAS, 343, 1327
Heavens A., Kitching T., Taylor A., 2006, astro-ph/0606568
Heavens A.F., Refregier A., Heymans C.E.C., 2000, MNRAS, 319, 649
Heavens A.F., Taylor A.N., 1995, MNRAS, 275, 483
Hetterscheidt M., et al., 2006, astro-ph/0606571
Heymans C., Brown M., Heavens A., Meisenheimer K., Taylor A., Wolf C., 2004, MNRAS, 347, 895
Heymans, C.E.C., Heavens A.F., 2003, MNRAS, 339, 711
Hirata C. & Seljak U. 2004, Phys. Rev. D204, 3056
Hoekstra H., Yee H.K.C., Gladders M.D., 2002, ApJ, 577, 595
Hoekstra H., et al., 2006, ApJ, 647, 116
Hu W., 1999, ApJ, 522, 21
Hu W., 2002, Phys. Rev. D66, 3515
Hu W. & Jain B., 2004, Phys. Rev. D, 70, 043009
Hu W., & Tegmark M., 1999, ApJ, 514, 65
Hu W. & White M., 2001, ApJ, 554, 67
Huterer D., 2002, Phys. Rev. D, 65, 063001
Huterer D. et al., 2005, astro-ph/0506030
Ishak M., 2005, astro-ph/0501594
Ishak M., Hirata C. M., McDonald P. & Seljak U., 2004, Phys. Rev. D, 69, 083514
Ishak M., Upadhye A., Spergel D., 2006, PhRvD, 74, 3513
Jain B., Taylor A.N., 2003, Phys. Rev. Lett., 9, 1302
Jarvis M. et al., 2003, AJ, 125, 1014
Jarvis M., Jain B., Bernstein G. & Dolney D., 2005, astro-ph/0502243
Jing Y.P., 2002, MNRAS, 335, 89
Kaiser N., 2005, AAS, 207, 15004
Kaiser N., Squires G., Broadhurst T., 1995, ApJ, 449, 460
Kaiser N., Wilson G., & Luppino G. A., 2000, astro-ph/0003338
King L., Schneider P., 2002, A&A, 396, 411
Kuo C.L. et al., 2004, ApJ, 600, 32
Linder E.V., 2003, Phys. Rev. Lett., 90, 091301

- Linder E.V., Jenkins A., 2003, MNRAS, 346, 573
Ma Z., Hu W., Huterer D., 2005, astro-ph/0506614
Peebles P.J.E., 1980, The Large-Structure of the Universe, Princeton University Press, Princeton
Pearson T.J., et al., 2003, ApJ, 591, 556
Percival W.J., et al., 2001, MNRAS, 327, 1297
Percival W.J., et al., 2004, MNRAS, 353, 1201
Press W., 1993, Sci, 259, 1931
Ratra B., Peebles P.J.E., 1988, Phys. Rev. D37, 3406
Refregier A., 2003 ARAA, 41, 645
Rhodes J., et al., 2004, ApJ, 605, 29
Riess A.G. et al., 2001, ApJ, 560, 49
Santos M., et al., 2003, MNRAS, 341, 623
Seljak U., Zaldarriaga M., 1996, ApJ, 469, 437
Semboloni E., et al., 2006, A&A, 452, 51
Schrabback T., et al., 2006, astro-ph/0606611
Simon P., King L., Schneider P., 2004, A&A, 417, 873
Smith R.E. et al. 2003, MNRAS, 341, 1311
Song Y.-S. & Knox L. 2004, Phys. Rev. D, 70, 063510
Spergel D. et al, 2003, ApJS, 148, 175
Spergel D. et al, 2006, astro-ph/0603449
Tadros H. et al, 1995, MNRAS, 305, 527
Takada M. & Jain, B. 2004, MNRAS, 348, 897
Takada M., White M., 2004, ApJL, 601, 1
Taylor A., 2005, ADS, pdus, confE, 28
Taylor A., Kitching T., Bacon D., Heavens A., 2006, astro-ph/0606416
Tegmark M., Taylor A.N., Heavens A.F., 1997, ApJ, 480, 22
Van Waerbeke L. et al. 2000, A&A 358, 30
Verde L. et al., 2002, MNRAS, 335, 432
Wester W., 2005, ASPC, 339, 152
White M. 2004, Astropart. Phys., 22, 211
Wittman D., Tyson J. A., Kirkman D., Dell'Antonio I., & Bernstein G. 2000, Nature, 405, 143
Wolf C., et al., 2001, A&A, 377, 442
Wolf, Meisenheimer & Roeser, 2001, A&A, 365, 660
Wolf et al., 2004, A&A, 421, 913
Yeche C. et al, 2005, astro-ph/0507170
Zaldarriaga L., Seljak U., 2000, ApJS, 129, 431
Zhan H. & Knox L. 2005, Astrophys. J., 616, L75

APPENDIX A: REMOVAL OF SINGULAR MODES

In this Appendix we show how any singular (k, ℓ) modes can be removed from the covariance matrices used in the 3D cosmic shear likelihood analysis.

We begin with a square covariance matrix C which can be decomposed using a standard singular value decomposition (SVD) into

$$C = U W V^T, \quad (24)$$

where W is a diagonal matrix that contains the singular values. Note that U and V are eigenvector matrices of CC^T and that $U^{-1} = U^T$ and $V^{-1} = V^T$. Our covariance matrices are symmetric so that $U = V$ in this case. Now consider one of our data vectors $\hat{\gamma}_i^A(k, \ell)$ represented by \mathbf{x} which can be transformed to a new data vector \mathbf{y} via

$$\mathbf{y} = B\mathbf{x} \quad (25)$$

where B can be any, not necessarily square, transformation matrix. A new covariance can then be defined

$$C'_{ij} \equiv \langle y_i y_j \rangle = \langle B_{ik} x_k B_{jl} x_l \rangle = B_{ik} B_{jl} C_{kl}, \quad (26)$$

which implies that

$$C' = B C B^T. \quad (27)$$

The choice of transformation, in this case, is motivated by decomposing C using a Cholesky decomposition which yields $C = U W U^T = L L^T$, where $L = U W^{1/2}$. So we use $B = \tilde{W}^{-1/2} U^{-1}$ where $\tilde{W}^{-1/2} = W^{-1/2}$ except that the elements of the inverse W matrix $1/w_i$ have been replaced with zero if $(1/w_i) \geq (\text{threshold})$ where the threshold represents machine precision (see Press, 1993; Numerical Recipes). The matrix B now contains a band of values below which zeros remove any singular modes from either the data vector or the covariance matrix via equations (25) and (27).

The transformation is performed using a fiducial cosmology (the choice of this does not affect the results) to yield a transformation matrix B which is then used throughout. \mathbf{y} and C' replace \mathbf{x} and C in the likelihood analysis.